

Structural Studies and Photochromism of Mercury(II)–Iodo Complexes of (Arylazo)imidazoles

K. K. Sarker,[†] B. G. Chand,[†] K. Suwa,[‡] J. Cheng,[§] T.-H. Lu,[§] J. Otsuki,[‡] and C. Sinha*[†]

Department of Chemistry, Inorganic Chemistry Section, Jadavpur University, Kolkata-7000 032, India, Department of Materials and Applied Chemistry, College of Science and Technology, Nihon University, 1-8-4 Kanda Surugadai, Chiyoda-ku, Tokyo 101-8308, Japan, and Department of Physics, National Tsing Hua University, Hsinchu 300, Taiwan

Received July 3, 2006

Neat reaction between HgI_2 and 1-methyl-2-(phenylazo)imidazole (Pai-Me) under microwave irradiation has isolated a novel compound whose structure shows intercalated HgI_2 in the layers of Pai-Me. They exist independently in interpenetrated arrays. In a solution phase study, the same reaction has synthesized an iodo-bridged azoimidazole– Hg(II) complex, $[\text{Hg}(\text{RaaiR}')(\mu\text{-I})_2]$ ($\text{RaaiR}' = 1\text{-alkyl-2-(arylazo)imidazole}$). The structures have been characterized by X-ray diffraction studies. Chloro-bridged Hg(II) complexes of azoimidazoles, $[\text{Hg}(\text{RaaiR}')(\mu\text{-Cl})(\text{Cl})_2]$, are also known. These complexes upon irradiation with UV light show trans-to-cis isomerization. The reverse transformation, cis-to-trans isomerization, is very slow with visible light irradiation. Quantum yields ($\phi_{t\rightarrow c}$) of trans-to-cis isomerization are calculated, and the free ligand shows higher ϕ than their Hg(II) complexes. The cis-to-trans isomerization is a thermally induced process. The activation energy (E_a) of cis-to-trans isomerization is calculated by controlled temperature reaction. The E_a 's of free ligands are much higher than that of halo-bridged Hg(II) –azoimidazole complexes. Chloro-bridged Hg(II) complexes show lower E_a 's than those of iodo-bridged complexes. DFT calculation has been adopted to rationalize the experimental results.

1. Introduction

Despite extensive study, coordination chemistry has yet to achieve complete understanding of the mechanism of interaction between the metal ions and ligands. Attempts have been made to explain this problem from both theoretical and experimental techniques.^{1,2} The fundamental principle of the formation of a complex is the interaction between the central metal ion and ligands. Depending on the force of interaction, the strength of bond is defined. The directional bonds are covalent. Noncovalent bonding, viz., hydrogen bonds, C–H– π , and π – π interactions, provide rigidity to the main covalently bonded complex.^{3,4} The reaction conditions

(solvent, temperature, catalyst, etc.) and nature of reagents have profusely influenced the composition, stereochemistry, and molecular structure of the complexes. Exploration of the material properties of organic molecules and their metal complexes are needed to complete the understanding of the compounds. Confirmative structure demonstration is a definite proof of bonding theories. Measurements of the metric parameters of complexes provides concrete information about coordination. It is assumed that a recognized bond has a length less than that of the sum of the van der Waals radii of participating atoms.⁵ In this work we perform a reaction under two different reaction conditions: neat reaction; solution-phase reaction. A neat reaction under microwave treatment of the mixture of HgI_2 and 1-alkyl-2-(arylazo)-

* To whom correspondence should be addressed. E-mail: c_r_sinha@yahoo.com. Fax: 91-033-2413-7121.

[†] Jadavpur University.

[‡] Nihon University.

[§] National Tsing Hua University.

- (1) (a) Wilkinson, G., Gillard, R. D., McCleverty, J., Eds. *Comprehensive Coordination Chemistry*; Pergamon Press: Oxford, U.K., 1987; Vols. 1–7. (b) Steel, C.; Vogtel, F. In *Perspectives in Coordination Chemistry*; Williams, A. F., Merbach, A. E., Eds.; VCH: Weinheim, Germany, 1992.
- (2) Cais, M. *Progress in Coordination Chemistry*; American Elsevier: New York, 1968.

- (3) (a) Desiraju, G. R. *Crystal Engineering: The Design of Organic Solids*; Elsevier: Amsterdam, 1989. (b) Desiraju, G. R. In *The Crystals as a Supramolecular Entity*; Lehn, J. M., Ed.; John Wiley & Sons: Chichester, U.K., 1996; Vol. 2.
- (4) (a) Burrows, A. D.; Harrington, R. W.; Mahon, M. F.; Price, C. E. *J. Chem. Soc., Dalton Trans.* **2000** 3845. (b) Desiraju, G. R. *Angew. Chem., Int. Ed. Engl.* **1995**, *34*, 2311. (c) Lehn, J. M. *Supramolecular Chemistry*; VCH: Weinheim, Germany, 1995.
- (5) Cotton, F. A.; Wilkinson, G. *Advanced Inorganic Chemistry*, 5th ed.; John Wiley and Sons: New York, 1988.

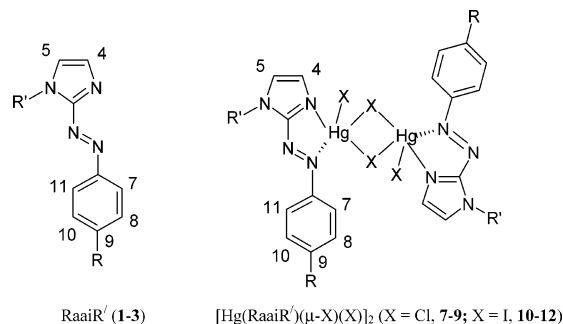
imidazoles (RaaiR') has synthesized a precoordination state of the complexes. The X-ray structure determination of one of the compounds shows that HgI₂ (metal compound) is intercalated in layers of ligand (1-methyl-2-(phenylazo)-imidazole, Pai-Me) and independently exists in interpenetrated arrays without showing covalent interaction. On the changing of reaction conditions, neat reaction to solution reaction, iodo-bridged coordination complexes [Hg(RaaiR')-(μ-I)(I)]₂ have been isolated. The complexes are characterized by spectroscopic (IR, UV–vis, NMR) data and by single-crystal X-ray diffraction studies. HgI₂ is chosen because of its efficient photoconductivity and has been used in radiographic and fluoroscopic medical imaging.

Toward the study of properties of the complexes, we have been interested to examine the photochromism of (arylazo)-imidazoles and the effect of metal coordination thereof. Photochromism is a reversible photoinduced transformation between two molecular states whose absorption spectra differ significantly.⁶ Incorporation of photochromic molecules into organic or hybrid organic–inorganic materials leads to development of very effective devices. Azo-conjugated metal complexes exhibit unique properties upon light irradiation in the area of photon-mode high-density information storage photoswitching devices.⁷ A combination of metal ions and π-conjugated systems with d–π electronic interaction might be used to realize novel optical, electronic, and magnetic properties.^{6–8} A preliminary report⁹ of the photochromism of 1-methyl-2-(phenylazo)imidazole (Pai-Me) has inspired us to examine this property on different other azoimidazoles and their metal complexes. In this work we examine photochromism of Pai-Et (1-ethyl-2-(phenylazo)imidazole), Tai-Me (1-methyl-2-(*p*-tolylazo)imidazole), Tai-Et (1-ethyl-2-(*p*-tolylazo)imidazole), and their chloro- and iodo-bridged Hg(II) complexes. The structural description of chloro-bridged complexes has been described previously.¹⁰ In this report HgI₂ intercalated into the layers of Pai-Me and iodo-bridged Hg(II)–azoimidazoles have been characterized by single-crystal X-ray diffraction studies.

2. Results and Discussion

2.1. Synthesis of Complexes. Two different reaction conditions have been employed for the synthesis of halomercury(II) compounds of 1-alkyl-2-(arylazo)imidazole (RaaiR': R = H, R' = Me (Pai-Me, **1a**); R = H, R' = Me (Pai-Me, **1a**); R = Me, R' = Me (Tai-Me, **1b**); R = H, R' = Et (Pai-Et, **2a**); R = Me, R' = Et (Tai-Et, **2b**); R = H, R' = CH₂Ph (Pai-CH₂Ph, **3a**); R = Me, R' = CH₂Ph (Tai-CH₂Ph, **3b**);

R = Me, R' = Me (Tai-Me, **1b**); R = H, R' = Et (Pai-Et, **2a**); R = Me, R' = Et (Tai-Et, **2b**); R = H, R' = CH₂Ph (Pai-CH₂Ph, **3a**); R = Me, R' = CH₂Ph (Tai-CH₂Ph, **3b**). Neat reaction between ligand (RaaiR') and HgI₂ under



microwave irradiation has synthesized a compound of composition [HgI₂][RaaiR']₂ (**4–6**) (a precoordination compound). The solution-phase reaction between HgX₂ (X = Cl, I) and RaaiR' in MeOH–2-methoxyethanol (2:1, v/v) has synthesized halo-bridged coordination complex of composition [Hg(RaaiR')(μ-X)(X)]₂ (X = Cl, **7–9**, and X = I, **10–12**). Under neat reaction condition of ligand and HgCl₂ by microwave irradiation, we have isolated only chloro-bridged product [Hg(RaaiR')(μ-Cl)(Cl)]₂ (**7–9**). The solution-phase reaction has also isolated chloro-bridged product. The structures of chloro-bridged compounds are previously described.¹⁰ The compounds are nonconducting, and their compositions have been supported by microanalytical data. The structures have been established in representative cases by single-crystal X-ray diffraction studies.

2.2. Molecular Structures. The crystals of (1-methyl-2-(phenylazo)imidazole)mercury(II) iodide (**4a**) were grown by slow evaporation of the THF extract of the solid-phase microwave-irradiated reaction. Diiodomercury(II)–1-methyl-2-(phenylazo)imidazole (**10a**) and diiodomercury(II)–1-benzyl-2-(*p*-tolylazo)imidazole (**12b**) were grown by slow evaporation of the reaction mixture in MeOH–2-methoxyethanol at ambient condition for 1 week.

2.2.a. Structure of [HgI₂][PaiMe]₂ (4a**).** The crystal structure of the complex is shown in Figure 1, and the bond parameters are listed in Table 1. The structure does not fit into our general conception of coordination complexes.^{1,5} Linear HgI₂ are intercalated into the layers of Pai-Me. The ligand exists as a weakly interacted π-dimer (Figure 1b): Ph(A)–Imz(B), 4.336(7) Å (symmetry: 1/2 – x, –1/2 + y, 1/2 – z); Ph(B)–Imz(A), 4.248(8) Å (symmetry: 1/2 – x, 1/2 + y, 1/2 – z) (where A and B represent two series of Pai-Me ligands in the dimer). Ph and Imz rings are connected by –N=N–, and they make dihedral angle of 7.9(3)°. The azo distance, –N=N–, of 1.245(6) Å is ~0.02 Å shorter than the previously reported free ligand value (1.261(2) Å).⁶ HgI₂ exists independently in the packing (Figure 1). However, weak interactions exist between Ph and Imz protons with Hg and I centers separately: C(1)–H(1)–Hg, 3.556(8) Å (symmetry: x, –y, 1/2 + z); C(6)–H(6)–Hg, 3.385(3) Å (–x, y, 1/2 – z); C(10)–H(10b)–I, 3.294(3) Å (–x, y, 1/2 – z). The presence of a C–H–π interaction also enhances the

- (6) Rau, H. *Photochromism: Molecules and Systems*; Durr, H., Bouas-Laurent, H., Eds.; Elsevier: Amsterdam, 1992; Chapter 4, pp 165–192. Brown, G. H. *Photochromism: Techniques of Chemistry*; Wiley-Interscience: New York, 1971; Vol. III.
- (7) Ire, M. *Chem. Rev.* **2000**, *100*, 1683. Ikeda, T.; Tsutsumi, O. *Science* **1995**, *268*, 1873. Kawata, S.; Kawata, Y. *Chem. Rev.* **2000**, *100*, 1777.
- (8) Nishihara, H. *Bull. Chem. Soc. Jpn.* **2004**, *77*, 407. Yutaka, T.; Mori, I.; Kurihara, M.; Mizutani, J.; Tamai, N.; Kawai, T.; Irie, M.; Nishihara, H. *Inorg. Chem.* **2002**, *41*, 7143.
- (9) Otsuki, J.; Suwa, K.; Narutaki, K.; Sinha, C.; Yoshikawa, I.; Araki, K. *J. Phys. Chem. A* **2005**, *109*, 8064.
- (10) Chand, B. G.; Ray, U. S.; Santra, P. K.; Mostafa, G.; Lu, T.-H.; Sinha, C. *Polyhedron* **2003**, *22*, 1205.

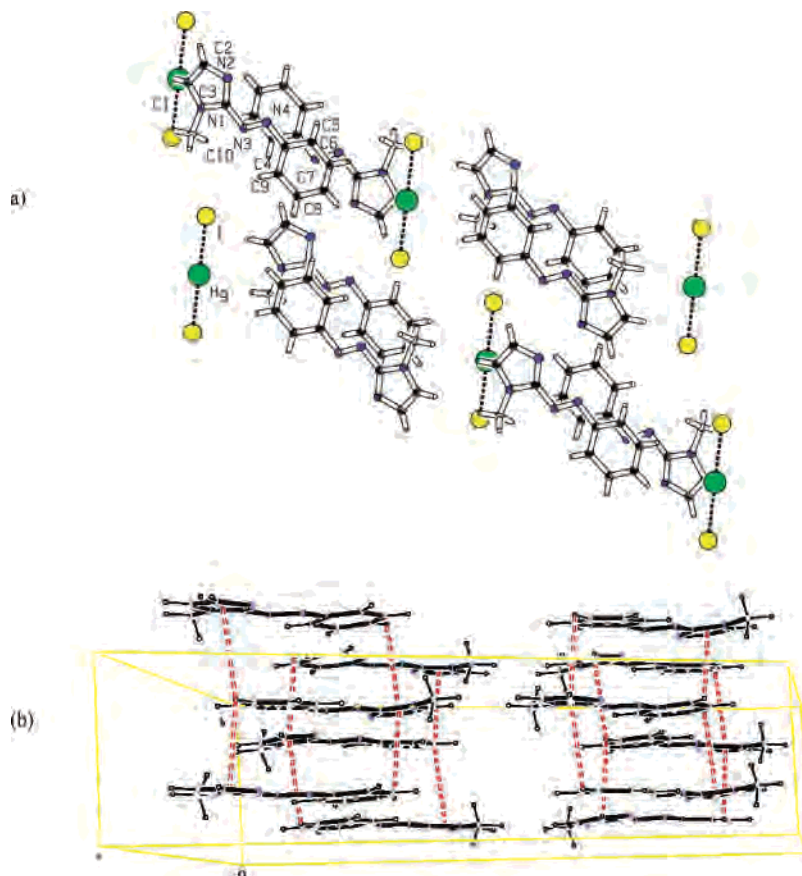


Figure 1. Unit cell of precoordination compound showing (a) interpenetrated layers of HgI₂ and Pai-Me and (b) π - π interaction of **4a**.

Table 1. Selected Bond Distances (Å) and Angles (deg) for [HgI₂][Haaime]₂ (**4a**)

bond distances		bond angles	
N(3)–N(4)	1.245(6)	I–Hg–I	179.99(2)
N(3)–C(3)	1.415(6)	N(3)–C(3)–N(1)	118.4(4)
N(4)–C(4)	1.443(5)	N(4)–N(3)–C(3)	112.9(4)
Hg–I(2)	2.8972(5)	N(3)–N(4)–C(4)	112.1(4)
		N(4)–C(4)–C(9)	122.3(4)
		N(4)–C(4)–C(5)	117.0(4)

strength between the dimers: C(7)–H(7)–Cg(1), 3.333(9) Å ($1/2 - x, 1/2 + y, 1/2 - z$) (Cg(1): C4–C5–C6–C7–C8–C9).

2.2.b. Structures of [Hg(Pai-Me)(μ -I)(I)]₂ (10a**) and [Hg(Tai-CH₂Ph)(μ -I)(I)]₂ (**12b**).** The molecular structures of [Hg(Pai-Me)(μ -I)(I)]₂ (**10a**) and [Hg(Tai-CH₂Ph)(μ -I)(I)]₂ (**12b**) are shown in Figure 2a,b, respectively. The bond parameters are listed in Table 2. Each discrete molecular unit consists of a dinuclear iodo-bridged Hg₂I₂ fragment. Pai-Me or Tai-CH₂Ph acts as an N,N'-donor end-capping agent, and a nonbridged I atom lies in a semiaxial position. The bridged Hg₂I₂ forms a unsymmetric tetraatomic rhombohedral plane (Hg–I(2), 2.7611(6) Å, and Hg–I(2)*, 3.1114(5) Å, in **10a** (* symmetry: $-x, -y, -z$); Hg–I(1), 2.6943(8) Å, and Hg–I(1)**, 3.3046(8) Å, in **12b** (** symmetry: $1 - x, 2 - y, 1 - z$)). The atomic arrangements Hg, N(4), C(1), N(1), N(3) (in **10a**) or Hg, N(1), C(3), N(3), N(4) (in **12b**) constitute chelate plane(s) with a maximum deviation <0.04 Å. The pendent aryl ring makes a small dihedral (13.5(3)° for **10a** and 8.6(2)° for **12b**) with the respective chelated azoimidazole ring. The bond angular values I(1)–Hg–I(2),

124.661(16)°, and I(1)–Hg–I(2)*, 103.787(15)°, for **10a** (* refers to symmetry $-x, -y, -z$) and I(1)–Hg–I(2), 137.98(3)°, and I(1)–Hg–I(2)*, 99.79(2)°, for **12b** (* refers symmetry $1 - x, 2 - y, 1 - z$) support for distorted geometry. Steric crowding of 1-CH₂Ph of **12b** may be the reason for larger deviation than **10a**, which bears the 1-Me group. The acute bite angle 62.66(3)° in **10a** is extended by Pai-Me or that of 64.9(3)° is extended by Tai-CH₂Ph in **12b** on coordination to Hg(II). The small chelate angle may be one of the reasons for geometrical distortion.^{10,11} The ligand (Pai-Me or Tai-CH₂Ph) is almost planar (maximum deviation <0.08 Å except for the 1-Me or 1-CH₂Ph group). The Hg–N(imidazole) (2.290(4) Å, **10a**; 2.302(9) Å, **12b**) is shorter than Hg–N(azo) (2.842(2) Å, **10a**; 2.739(7) Å, **12b**) which reflects stronger interaction between Hg(II) and N(imidazole). The Hg–N distances are longer than chloro-bridged Hg(II)–azoimidazole complexes (Hg–N(imidazole), 2.204(5), and Hg–N(azo), 2.757(5) Å).^{10,11} Although the Hg–N(azo) bond length is very long, it is less than the sum of the van der Waals radii of Hg(II) (1.55 Å) and N(sp²) (1.53 Å). This implies significant bonding interaction between these components. Strong coordination of imidazole-N to Hg(II) has significant biochemical implications and explains the great toxicity of Hg(II).¹² Weak and flexible bonds are very effective to induce some functional property in the mol-

(11) Chand, B. G.; Ray, U. S.; Cheng, J.; Lu, T.-H.; Sinha, C. *Inorg. Chim. Acta* **2005**, *358*, 1927.

(12) Fergusson, J. E. *The heavy elements: chemistry, environment impact and health effects*; Pergamon: Oxford, U.K., 1990.

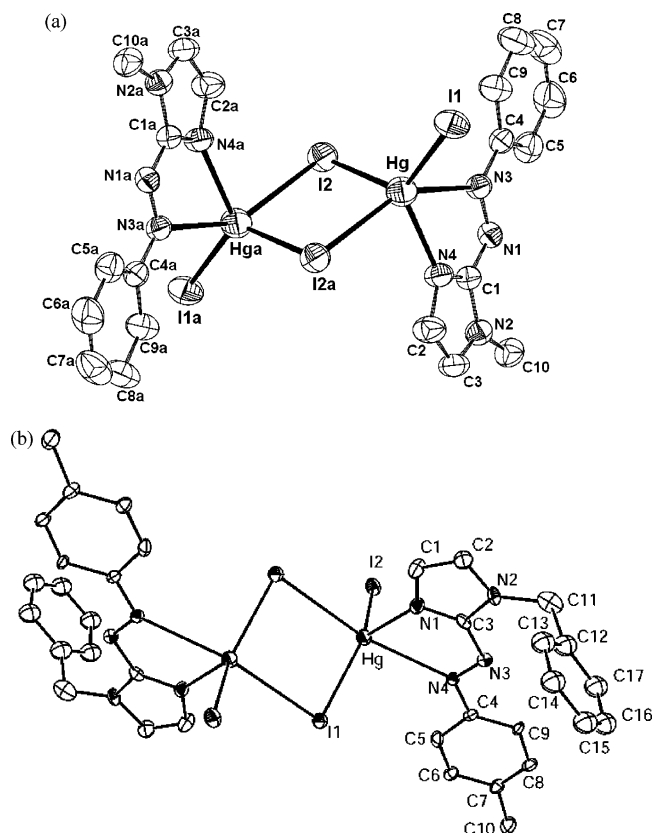


Figure 2. Molecular structures of iodo-bridged dimers: (a) $[\text{Hg}(\text{Pai-Me})(\mu\text{-I})(\text{I})_2]$ (**10a**); (b) $[\text{Hg}(\text{Tai-CH}_2\text{Ph})(\mu\text{-I})(\text{I})_2]$ (**12b**).

Table 2. Selected Bond Distances (Å) and Angles (deg) for $[\text{Hg}(\text{Pai-Me})(\mu\text{-I})(\text{I})_2]$ (**10a**) and $[\text{Hg}(\text{Tai-CH}_2\text{Ph})(\mu\text{-I})(\text{I})_2]$ (**12b**)

bond distances		bond angles	
$[\text{Hg}(\text{Pai-Me})(\mu\text{-I})(\text{I})_2]$ (10a)			
Hg–I(1)	2.6441(5)	I(1)–Hg–I(2)	124.661(16)
Hg–I(2)	2.7611(6)	I(1)–Hg–I(2) ^a	103.787(15)
Hg–I(2) ^a	3.1114(5)	N(4)–Hg–I(1)	123.89(13)
Hg–N(4)	2.290(4)	N(4)–Hg–I(2)	107.67(12)
Hg–N(3)	2.842(2)	N(4)–Hg–I(2) ^a	89.86(12)
N(1)–C(1)	1.382(7)	I(2)–Hg–I(2) ^a	94.324(13)
N(3)–C(4)	1.434(7)	Hg–I(2)–Hg ^a	85.676(13)
N(1)–N(3)	1.262(6)	N(3)–Hg–I(1)	100.63(4)
		N(3)–Hg–I(2)	85.01(2)
		N(3)–Hg–N(4)	62.66(3)
$[\text{Hg}(\text{Tai-CH}_2\text{Ph})(\mu\text{-I})(\text{I})_2]$ (12b)			
Hg–I(1)	2.6943(8)	I(1)–Hg–I(2)	137.98(3)
Hg–I(2)	2.6406(8)	I(1)–Hg–I(2) ^b	99.79(2)
Hg–N(1)	2.302(9)	I(1)–Hg–I(1) ^b	89.69(2)
Hg–N(4)	2.739(7)	N(1)–Hg–I(1)	114.15(18)
Hg–I(1) ^b	3.3046(8)	N(1)–Hg–I(2)	107.23(18)
N(3)–C(3)	1.426(11)	N(1)–Hg–N(4)	64.9(3)
N(4)–C(4)	1.385(9)	I(2)–Hg–N(4)	98.86(15)
N(3)–N(4)	1.272(9)	I(1)–Hg–N(4)	92.24(15)
		N(1)–Hg–I(1) ^b	86.8(2)
		N(4)–Hg–I(1)	149.70(19)
		Hg–I(1)–Hg ^b	90.31(2)

^a Symmetry: $-x, -y, -z$. ^b Symmetry: $1-x, 2-y, 1-z$.

ecules.¹³ The weak bonding interaction between the Mn(II) and N(azo) center in $[\text{Mn}(\text{N}_3)_2(\text{TaiEt})]_n$ (TaiEt = 1-ethyl-2-(*p*-tolylazo)imidazole) is responsible for structural distur-

tion and hence the canting phenomenon and remnant magnetism.¹⁴ Because of the long Hg(II)–N(azo) distance, the molecule may exhibit photophysical activation via cleavage of this bond followed by rotation to introduce photoisomerization. In fact, we have examined photochromism of these molecules (vide infra). The N=N distance is 1.262(6) Å in **10a** and 1.272(9) Å in **12b**. The Hg–I(bridged) (Hg–I(2), 2.7611(6) Å, in **10a** and Hg–I(1), 2.6943(8) Å, in **12b**) distance is longer than the Hg–I(nonbridged) (Hg–I(1), 2.6441(5) Å, in **10a** and Hg–I(2), 2.6406(8) Å, in **12b**) bond length. The bond parameters are in corroboration with previously reported data.^{10,11} Hg–I(1) in **10a** and Hg–I(2) in **12b** are in semiaxial positions in their respective planes. The chelate ring around Hg is twisted in a manner so that the Hg–N(azo) inclines toward the axial Hg–I bond [N(3)–Hg–I(1), 100.63(3)°, and N(4)–Hg–I(1), 123.9(1)°, in **10a** and N(4)–Hg–I(2), 98.86(15)°, and N(1)–Hg–I(2), 107.23(18)°, in **12b**].

A π – π interaction (imidazole–phenyl, 4.15(1) Å; symmetry, $-x, -y, 1-z$) in **10a** between imidazole and phenyl rings with the partners of neighboring molecule has generated a supramolecular arrangement (Figure 3). The presence of C–H– π (2.772 Å; symmetry $3/2-x, -1/2+y, 1/2-z$; between imidazole C–H and the pendent *p*-tolyl ring of neighboring molecule) and π – π interactions (4.103 Å; symmetry $1-x, -y, -z$; between imidazole and *p*-tolyl rings of neighboring molecules) in **12b** have generated a 1-D supramolecule.

2.3. Spectral Studies. IR spectra of $[\text{Hg}(\text{RaaiR}')(\mu\text{-X})(\text{X})_2]$ (**7–12**) exhibit $\nu(\text{C}=\text{N})$ and $\nu(\text{N}=\text{N})$ at 1580–1600 and 1375–1380 cm^{-1} , respectively, and are shifted to lower frequency by 15–20 cm^{-1} with reference to the free ligand values.^{10,15} Precoordination compounds $[\text{HgI}_2][\text{RaaiR}'_2]$ (**4–6**) exhibit hardly any shift of N=N and C=N frequencies compared to the free ligand values.¹⁵ This, in fact, helps us to comment on the no-coordination situation of N-donor centers of the ligand with Hg(II). This is also supported from the X-ray crystal structure study (Figure 1).

The solution electronic spectra of **7–12** were recorded in MeCN in 200–900 nm. There are four bands in the UV–vis region, and three of them are intense ($\epsilon \sim 10^4 \text{ mol}^{-1} \text{ dm}^3 \text{ cm}^{-1}$) at 255–270, 350–365, and 380–390 nm. On comparing with free ligand spectra¹⁵ and that of the chloro-bridged Hg(II) complex,¹⁰ we may conclude that they are coming from intramolecular charge-transfer transitions ($n-\pi^*$, $\pi-\pi^*$), which is also supported by frontier molecular orbital calculations using X-ray diffraction parameters (vide supra). The fourth band appears at 435–445 nm in the case of **7–12** and is weak in intensity ($\epsilon \sim 10^3 \text{ mol}^{-1} \text{ dm}^3 \text{ cm}^{-1}$). This may refer to Hg(II) $\rightarrow \pi^*$ (azoimine) charge-transfer transitions.^{10,11}

The ¹H NMR spectra of the complexes are recorded in CDCl₃, and the signals are assigned (Table 3) unambiguously

(14) Ray, U. S.; Ghosh, B. K.; Monfort, M.; Ribas, J.; Mostafa, G.; Lu, T.-H.; Sinha, C. *Eur. J. Inorg. Chem.* **2004**, 250.

(15) Misra, T. K. Ph.D. Thesis. *Transition Metal Chemistry of 2-(Arylazo)imidazoles: Synthesis, Characterisation and Electrochemical Studies*; Burdwan University: Burdwan, India, 1999.

(13) Kepert, C. J. *Chem. Commun.* **2006**, 695. Nathan C.; Gianneschi, M.; Masar, S., III; Mirkin, A. *Acc. Chem. Res.* **2005**, *38*, 825.

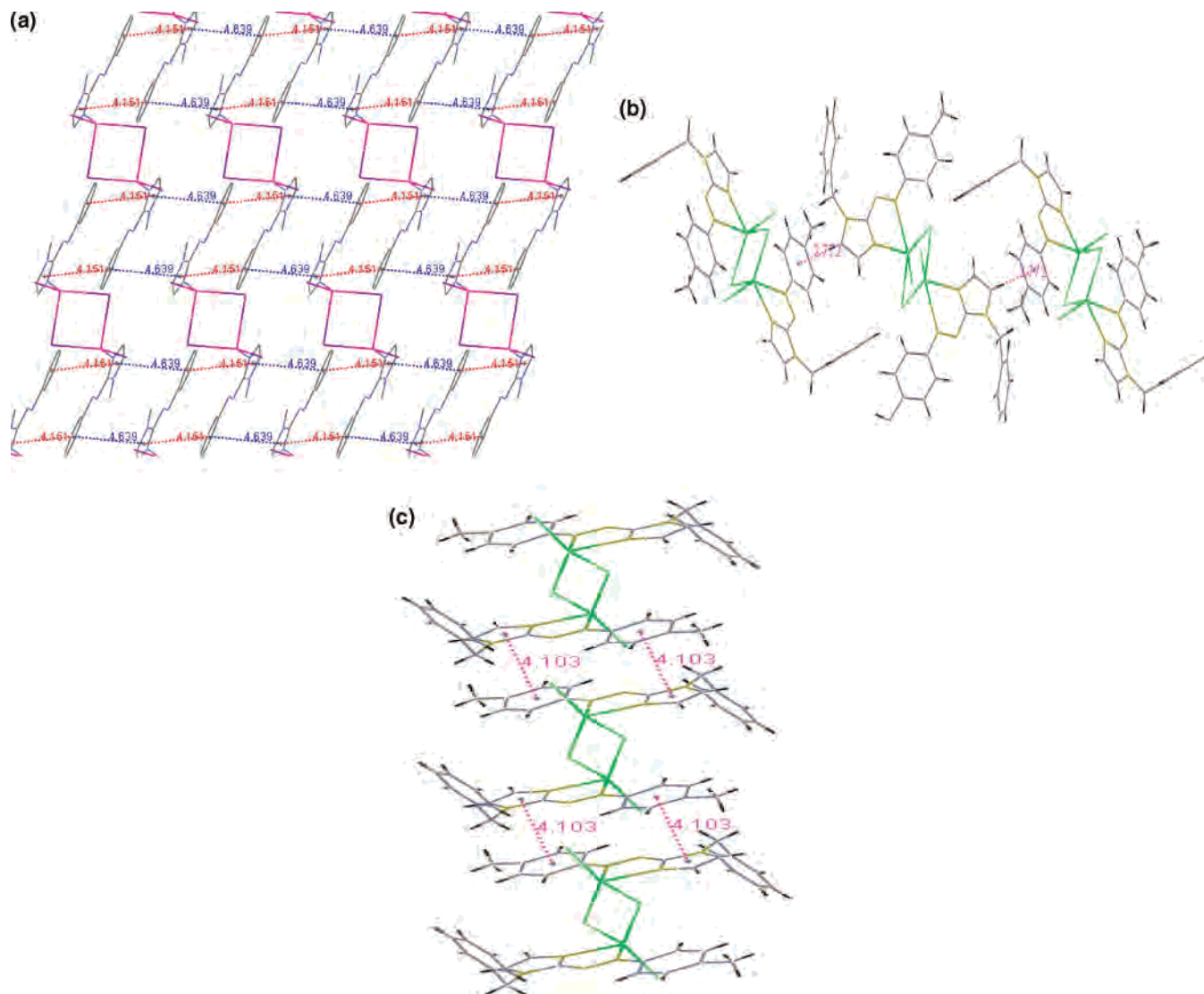


Figure 3. (a) Intermolecular π - π interactions in **10a** (red, Ring2-Ring1#2; blue, Ring2-Ring1#1). (b) C-H- π (a) and π - π (b) interactions in the dimeric unit of [Hg(Tai-CH₂Ph)(μ -I)(I)]₂ (**12b**).

Table 3. ¹H NMR Spectral Data for Hg(II) Complexes (**4–6** and **10–12**) in CDCl₃ at 300 K

compd	δ (ppm) (J (Hz))								
	4-H ^a	5-H ^a	7,11-H ^b	8,10-H ^b	9-R	1-CH ₃ ^e	1-CH ₂	(1-CH ₂)CH ₃	Ph-H
4a	7.13	7.00	7.55 (7.2)	7.50 ^c	7.50 ^d	4.03			
4b	7.07	6.95	7.53 (7.2)	7.33 (7.0)	2.40 ^f	4.04			
5a	7.22	7.11	7.60 (7.8)	7.43 ^c	7.03 ^d		4.53 ^g (12.0)	1.59 ^h (7.0)	
5b	7.19	7.06	7.48 (7.2)	7.30 (7.0)	2.45 ^f		4.52 ^g (12.0)	1.53 ^h (7.0)	
6a	7.24	7.09	7.69 (7.2)	7.49 ^c	7.49 ^d		5.53 ^e		7.30–7.40
6b	7.22	7.14	7.65 (7.2)	7.32 (7.2)	2.40 ^f		5.52 ^e		7.30–7.45
10a	7.30	7.24	8.09 (7.0)	7.57 ^c	7.57 ^d	4.14			
10b	7.37	7.26	8.00 (7.0)	7.48 (7.0)	2.48 ^f	4.13			
11a	7.36	7.25	8.05 (7.0)	7.50 ^c	7.50 ^d		4.63 ^g (10.0)	1.58 ^h (7.5)	
11b	7.37	7.21	8.02 (7.0)	7.32 (7.0)	2.40 ^c		4.58 ^g (12.0)	1.55 (7.5)	
12a	7.45	7.31	8.00 (7.0)	7.55 ^c	7.55 ^d		5.73 ^e		7.30–7.40
12b	7.44	7.26	7.93 (7.0)	7.39 (7.0)	2.40 ^f		5.77 ^e		7.30–7.40

^a Broad singlet. ^b Doublet. ^c Multiplet. ^d δ (9-H). ^e Singlet. ^f δ (9-Me). ^g Quartet.

by spin-spin interaction, the effect of substitution therein, and on comparing previously reported cases.^{10,11} The atom-numbering pattern is shown in the structure. Data reveal that the signals in the spectra of **10–12** in general are shifted downfield compared to those of the the spectra of the free ligand.¹⁵ The signal pattern and chemical shift data in the

spectra of **4–6** are similar to those of the free ligand. This supports that the ligand is coordinated to Hg(II) in **10–12** and not in the case of **4–6**. The 7,11-H's are shifted to higher δ by ~ 0.5 ppm when we move from **4–6** to **10–12**. This observation supports the existence of strong interaction between ligands and Hg(II) in **10–12** compared to **4–6**. An

important feature of the spectra of **10**–**12** with their chloro-analogue $[\text{Hg}(\text{RaaiR}')(\mu\text{-Cl})(\text{Cl})_2]^{10}$ is the shifting of imidazole protons, 4-H and 5-H, to higher δ values (by >0.2 ppm), while aryl protons (7-H–11-H) remain almost at the same signal positions. This is because iodo makes mercury(II) softer¹⁶ in the Hg–I (**10**–**12**) system than chloro in $[\text{Hg}(\text{RaaiR}')(\mu\text{-Cl})(\text{Cl})_2]$ (**7**–**9**). Thus, Hg(II) prefers to bind imidazole-N more efficiently in the present case than that of $[\text{Hg}(\text{RaaiR}')(\mu\text{-Cl})(\text{Cl})_2]$. Aryl signals are shifted to the lower field side on Me-substitution to the aryl ring. This is due to the electron-donating effect of the Me– group. N(1)–R' shows the usual signal pattern as earlier.¹⁰

2.4. Photochromism of Ligands and Complexes. The trans-to-cis isomerization of Tai-Me (**1b**), Pai-Et (**2a**), and Tai-Et (**2b**), chloro-bridged $[\text{Hg}(\text{Pai-Me})(\mu\text{-Cl})(\text{Cl})_2]$ (**7a**), $[\text{Hg}(\text{Tai-Me})(\mu\text{-Cl})(\text{Cl})_2]$ (**7b**), $[\text{Hg}(\text{Pai-Et})(\mu\text{-Cl})(\text{Cl})_2]$ (**8a**), and $[\text{Hg}(\text{Tai-Et})(\mu\text{-Cl})(\text{Cl})_2]$ (**8b**), and iodo-bridged-Hg(II) $[\text{Hg}(\text{Pai-Me})(\mu\text{-I})(\text{I})_2]$ (**10a**), $[\text{Hg}(\text{Tai-Me})(\mu\text{-I})(\text{I})_2]$ (**10b**), $[\text{Hg}(\text{Pai-Et})(\mu\text{-I})(\text{I})_2]$ (**11a**), and $[\text{Hg}(\text{Tai-Et})(\mu\text{-I})(\text{I})_2]$ (**11b**) have been investigated. The photochromism of Pai-Me is reported earlier.⁹ The complexes $[\text{Hg}(\text{Pai-CH}_2\text{Ph})(\mu\text{-X})(\text{X})_2]$ (X = Cl, **9a**, and X = I, **12a**) and $[\text{Hg}(\text{Tai-CH}_2\text{Ph})(\mu\text{-X})(\text{X})_2]$ (X = Cl, **9b**, and X = I, **12b**) are very sluggish to change their absorption spectra upon UV light irradiation and have not been studied further. The photoisomerization of ligand in the complexes is dependent on the nature of the metal ion and its oxidation state.⁸ To investigate possible modulation of photochromes by metal ions, we carried out some experiments with metal ions added to a methanol solution of Pai-Me.⁹ The addition of Cu(II), Zn(II), and Ag(I) to Pai-Me solution has shifted the absorption spectra to longer wavelengths. The illumination at the $\pi\text{-}\pi^*$ peak (355 nm) isomerizes *trans*-Pai-Me to *cis*-Pai-Me, and subsequent illumination at 454 nm reversed the course of reaction. The chelate complexes of these metal ions are structurally known.^{17–19} Herein, we are investigating photoisomerization of Hg–RaaiR' complexes in the presence of chloride (Cl^-) and iodide (I^-). Iodide is chosen because of its light-sensitive oxidative reactions²⁰ intending its participation in the experimental process. It is observed that upon irradiation with UV light trans-to-cis photoisomerization proceeded and the cis molar ratio reached $>95\%$. The absorption spectra of the trans ligands (Pai-Et, Tai-Me, Tai-Et) in toluene changed with isosbestic points upon excitation (Figures 4 and 5) into the cis isomer and also in the case of the respective complexes. The ¹H NMR technique has been adopted to

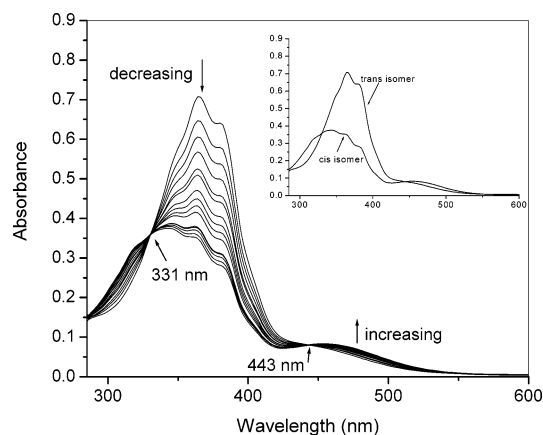


Figure 4. Spectral changes of Tai-Me in toluene upon repeated irradiation at 365 nm at a 3 min interval at 25 °C. The inset figure shows spectra of the cis and trans isomers of Tai-Me.

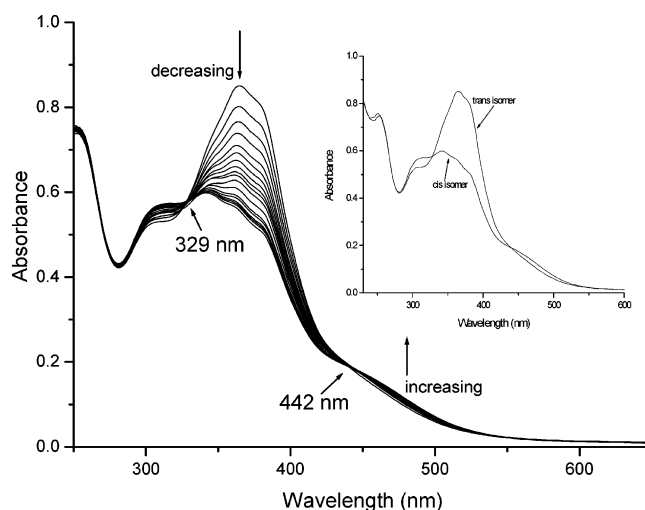


Figure 5. Spectral changes of $[\text{Hg}(\text{Tai-Me})(\mu\text{-I})_2]$ in MeCN upon repeated irradiation at 367 nm at a 3 min interval at 25 °C. The inset figure shows spectra of the cis and trans isomers of the complex.

measure the percentage composition of the irradiated solution, which supports the composition obtained from absorption spectra. The ¹H NMR signals of the aromatic ring protons are significantly shifted to the upfield portion after light irradiation. The ligands and complexes show little sign of degradation upon repeated irradiation at least up to 15 cycles in each case. We have also examined the UV-light irradiation behavior of green *tcc*-Ru(Pai-Me)₂Cl₂ and blue *ctc*-Ru(Pai-Me)₂Cl₂²⁰ in MeCN. Ruthenium(II) complexes are silent to photoisomerization. There may be several reasons on the basis of structure and energy ordering of the participating functions. Pai-Me is chelated to Ru(II), and the X-ray structure determination shows that the Ru–N(azo) bond length is shorter than Ru–N(imidazole) distances. This has also prompted charge flow $d\pi(\text{Ru}) \rightarrow \pi^*(\text{azo})$ which synergistically enhances Ru–N(azo) bond strength. This structural rigidity may resist photoisomerization. Besides, the energy transfer from $\pi\text{-}\pi^*$ to the MLCT state may cause very fast bleaching.²² The structures of Hg(II)–RaaiR' halo complexes (vide supra) (Figure 2) show very long Hg(II)–N(azo) bond distances¹⁰ compared to Hg–N(imidazole) distances. Upon UV-light irradiation the Hg–N(azo) bond

- (16) Softening, I.; Wang, X.; Knobler, C. B.; Zebeng, Z.; Hawthorne, M. F. *J. Am. Chem. Soc.* **1994**, *116*, 7142. Pauling, L. *The Nature of the Chemical Bond*, 3rd ed.; Cornell University Press: Ithaca, NY, 1960.
- (17) Ray, U. S.; Banerjee, D.; Mostafa, G.; Lu, T.-H.; Sinha, C. *New J. Chem.* **2004**, *28*, 1432.
- (18) Chand, B. G.; Ray, U. S.; Mostafa, G.; Lu, T.-H.; Sinha, C. *J. Coord. Chem.* **2004**, *57*, 627. Chand, B. G.; Ray, U. S.; Cheng, J.; Lu, T.-H.; Sinha, C. *Polyhedron* **2003**, *22*, 1213.
- (19) Dinda, J.; Jasimuddin, Sk.; Mostafa, G.; Hung, C. H.; Sinha, C. *Polyhedron* **2004**, *23*, 793.
- (20) O'Regan, B.; Moser, J.; Anderson, M. *J. Phys. Chem.* **1990**, *94*, 8720. Fitzmaurice, D. J.; Esche, M.; Frei, H.; Moser, J. *J. Phys. Chem.* **1993**, *97*, 3806.
- (21) Misra, T. K.; Das, D.; Sinha, C.; Ghosh P. K.; Pal, C. K. *Inorg. Chem.* **1998**, *37*, 1672.

Table 4. Excitation Wavelength (λ_{π,π^*}), Rate of Trans (t) \rightarrow Cis (c) Conversion and Quantum Yield ($\phi_{t\rightarrow c}$)

compd	λ_{π,π^*} (nm)	isosbestic point(s) (nm)	rate of t \rightarrow c conversn $\times 10^8$ (s $^{-1}$)	$\phi_{t\rightarrow c}$
Pai-Me (1a)	363	333, 431	5.06	0.25 \pm 0.03
Tai-Me (2a)	365	331, 443	3.70	0.218 \pm 0.007
Pai-Et (1b)	364	333, 434	4.83	0.241 \pm 0.012
Tai-Et (2b)	365	328, 444	4.59	0.206 \pm 0.006
[Hg(Pai-Me)(μ -Cl)Cl] ₂ (7a)	363	333, 447	3.21	0.181 \pm 0.020
[Hg(Tai-Me)(μ -Cl)Cl] ₂ (7b)	365	348, 438	3.43	0.157 \pm 0.010
[Hg(Pai-Et)(μ -Cl)Cl] ₂ (8a)	367	342, 449	3.19	0.162 \pm 0.020
[Hg(Tai-Et)(μ -Cl)Cl] ₂ (8b)	369	343, 458	3.49	0.144 \pm 0.010
[Hg(Pai-Me)(μ -I)I] ₂ (10a)	367	336, 452	4.20	0.211 \pm 0.011
[Hg(Tai-Me)(μ -I)I] ₂ (10b)	367	329, 442	3.22	0.177 \pm 0.009
[Hg(Pai-Et)(μ -I)I] ₂ (11a)	368	341, 449	3.28	0.202 \pm 0.016
[Hg(Tai-Et)(μ -I)I] ₂ (11b)	371	345, 462	3.63	0.197 \pm 0.010

may cleave easily to make a free rotatory azo-aryl group which isomerizes to the cis form. The quantum yields were measured for the trans-to-cis ($\phi_{t\rightarrow c}$) photoisomerization of these compounds in toluene (free ligand)/MeCN (complexes) on irradiation of UV wavelength (Table 4). The $\phi_{t\rightarrow c}$ values are significantly dependent on the nature of substituents and are less so than that of Pai-Me ($\phi_{t\rightarrow c} = 0.25 \pm 0.03$). The Me substituent at the azophenyl group (Pai-R' (**1**) to Tai-R' (**2**)) and Et substituent at the N(1)-position (1-Me (**a**) to 1-Et (**b**)) both reduce $\phi_{t\rightarrow c}$ values. The effect is significant for the Tai-R' ligand. Thus, the Me substituent at the $-N=N-$ phenyl group reduces the rate of isomerization (Table 5). In the complexes [Hg(Rai-R')(μ -X)(X)]₂ (X = Cl for **7** and **8** and X = I for **10** and **11**) the $\phi_{t\rightarrow c}$ values are significantly less than that of free ligand data. Two reasons may be considered for this decrement: (i) the presence of the coordinated HgX₂ motif heavily increases the molecular weight of the complex unit which may severely interfere with the motion of the $-N=N-Ar$ moiety; (ii) the photobleaching efficiency of a heavy atom like Hg(II) and the iodo group²³ may snatch out energy from the $\pi-\pi^*$ excited state and may cause very fast deactivation other than the photochromic route. One should note that the rotor volume has significant influence on the isomerization rate and quantum yields.^{8,22} The complexation increases the rotor volume leading to a less efficient isomerization.

Thermal cis-to-trans isomerizations of the ligands (**1b**, **2a**, **2b**) and complexes (**7**, **8**, **10**, **11**) were followed by UV-vis spectroscopy in toluene (ligands)/MeCN (complexes) at varied temperatures, 298–313 K. The Arrhenius plots in the range 298–313 K gave a linear graph from which the activation energies were obtained (Table 6, Figure 6). The E_a 's of free ligands are closer to that of Pai-Me but lower than that of azobenzene. In the complexes **7**, **8**, **10**, and **11**, the E_a 's are severely reduced, which means faster cis-to-trans thermal isomerization of the complexes. The entropies of activation (ΔS^\ddagger) are more negative in the complexes than

that of the free ligand. This is also in support of an increase in rotor volume in the complexes. The chloro complexes (**7**, **8**) have slightly lower activation energy (lowered by 3–8 kJ mol⁻¹, Table 4) than that of iodo-bridged complexes (**10**, **11**), which are also in agreement with lower quantum yields in the former (Table 5).

2.5. DFT Calculation and Correlation with Spectral Properties. Density functional theory was employed to obtain insight into the electronic structure of the mercury complexes of (arylozo)imidazoles. The calculations for **10a** were conducted on using the coordinates of the crystal structure obtained in this work and were compared with the results obtained for the ligand, **1a**. Although the DFT calculations on **1a** have been reported previously,⁹ we have calculated them again using the same functionals and basis functions as for **10a** to compare the results. The results obtained here for **1a** using B3LYP with LanL2DZ for Hg and MIDI! for other elements are qualitatively consistent with those obtained previously using the B88 and LYP functionals and the DZVP basis set.

The major results of the calculations are graphically illustrated in Figure 7. For **1a**, the LUMO is π^* , which is delocalized over the entire conjugated system. The HOMO and HOMO-1 are close in energy. A π orbital is dominant in the HOMO, but the n orbitals on the azo nitrogens also contribute. This mixing occurs probably because of the slight nonplanarity of the crystal structure of **1a**, on which the calculations were based. Meanwhile, the azo n orbitals are major contributors to the HOMO-1. The LUMO in **10a** is on the Pai-Me ligand, and the symmetry of the orbital is the same as the LUMO of **1a**. On the other hand, the occupied frontier orbitals are dominated by the π orbitals of iodines with some contributions from the d orbitals of mercury and the azo n orbitals from the ligands. The ligand π orbital of a symmetry similar to that of the HOMO of **1a** is found below these iodine-centered orbitals (MO no. 206). Further below in energy, an orbital with a major contribution from the azo n orbitals is found (MO no. 204). By complexation with mercury ion, the unoccupied and occupied frontier orbitals in that part of the ligand are stabilized to a similar extent. Also the symmetries of the orbitals are largely retained upon complexation. These results explain the experimental results that there is little shift in λ_{\max} in the absorption spectra and that the photochromic activity is well retained in the complex.

(22) Yutaka, T.; Kurihara, M.; Nishihara, H. *Mol. Cryst. Liq. Cryst.* **2000**, *343*, 193. Yutaka, T.; Mori, L.; Kurihara, M.; Mizutani, J.; Kubo, K.; Furusho, S.; Matsumura, K.; Tamai, N.; Nishihara, H. *Inorg. Chem.* **2001**, *40*, 4986.

(23) Zhao, X.; Chan, W.; Wong, M.; Xiao, D.; Li, Z. *Am. Lab.* **2003**, *13*. Hutton, A. T.; Irving, H. M. N. H. *J. Chem. Soc., Dalton Trans.* **1982**, 2299. Zentai, G.; Partain, L.; Pavlyuchkova, R.; Proano, C.; Virshup, G.; Melekshov, L.; Zuck, A.; Breen, B. N.; Dagan, O.; Vilensky, A.; Schieber, M.; Gilboa, H.; Bennet, P.; Shah, K.; Dimitriev, Y.; Thomas, J.; Yaffe, M.; Hunter, D. *Proc. SPIE* **2003**, *5030* (June).

Table 5. Rate and Activation Parameters for Cis (c) → Trans (t) Thermal Isomerization

compd	temp (K)	rate of thermal c → t conversn × 10 ⁵ (s ⁻¹)	E _a (kJ mol ⁻¹)	ΔH [*] (kJ mol ⁻¹)	ΔS [*] (J mol ⁻¹ K ⁻¹)	ΔG [*] (kJ mol ⁻¹)
Pai-Me (1a) ^{a,d}	298	2.2	79.0	77.05	-77.1	100.00
	303	4.0				
	313	8.8				
	323	27.5				
Tai-Me (1b) ^a	298	7.3	87.57	85.03	-38.84	96.60
	303	12.0				
	308	26.0				
	313	37.0				
Pai-Et (2a) ^a	298	3.3	86.87	84.33	-47.83	98.58
	303	5.8				
	308	9.7				
	313	18.0				
Tai-Et (2b) ^a	298	6.4	87.63	87.08	-40.20	97.06
	303	9.8				
	308	18.7				
	313	34.0				
[Hg(Pai-Me)(μ-Cl)Cl] ₂ (7a)	298	22.3	32.31	29.77	-214.65	93.73
	303	29.9				
	308	35.1				
	313	42.3				
[Hg(Tai-Me)(μ-Cl)Cl] ₂ (7b)	298	34.3	27.82	25.28	-226.36	92.73
	303	41.9				
	308	49.7				
	313	58.9				
[Hg(Pai-Et)(μ-Cl)Cl] ₂ (8a)	298	48.3	28.58	26.04	-220.84	91.85
	303	61.0				
	308	73.1				
	313	84.2				
[Hg(Tai-Et)(μ-Cl)Cl] ₂ (8b)	298	56.7	27.42	24.88	-223.49	91.48
	303	69.6				
	308	82.1				
	313	96.7				
[Hg(Pai-Me)(μ-I)I] ₂ ^b (10a)	298	21.6	40.89	38.36	-186.20	93.85
	303	30.0				
	308	37.1				
	313	48.4				
[Hg(Tai-Me)(μ-I)I] ₂ ^b (10b)	298	41.4	30.97	28.43	-214.1	92.24
	303	53.3				
	308	61.7				
	313	79.3				
[Hg(Pai-Et)(μ-I)I] ₂ ^b (11a)	298	50.6	35.53	32.99	-197.53	91.69
	303	59.0				
	308	79.9				
	313	98.3				
[Hg(Tai-Et)(μ-I)I] ₂ ^b (11b)	298	76.7	36.00	34.12	-190.21	90.81
	303	92.6				
	308	124.0				
	313	143.2				

^a In toluene. ^b In acetonitrile. ^c At 298 K. ^d Reference 9.

3. Experimental Section

3.1. Materials. HgI₂ was obtained from Loba Chemicals, Bombay, India. 1-Alkyl-2-(arylazo)imidazoles were synthesized by reported procedure.²¹ All other chemicals and solvents were reagent grade as received.

3.2. Physical Measurements. Microanalytical data (C, H, N) were collected on a Perkin-Elmer 2400 CHNS/O elemental analyzer. Spectroscopic data were obtained using the following instruments: UV–vis spectra from a Perkin-Elmer Lambda 25 spectrophotometer; IR spectra (KBr disk, 4000–200 cm⁻¹) from a Perkin-Elmer RX-1 FTIR spectrophotometer; luminescence studies from a Perkin-Elmer LS-55 spectrofluorometer; ¹H NMR spectra from a Bruker (AC) 300 MHz FTNMR spectrometer.

3.3.a. Synthesis of [HgI₂][HaaiMe]₂ (4a**).** A finely powdered mixture of 1-methyl-2-(phenylazo)imidazole (Pai-Me, **1a**) (0.5 g, 2.69 mmol) and HgI₂ (0.25 g, 0.55 mmol) was taken in a Teflon reactor (100 mL capacity) and placed in microwave oven of 450 W for 5 min × 3 with a 5 min interval at each step. The reactor was then cooled, and the solution was filtered and evaporated slowly

in air. Orange-red crystals were separated. They were collected by filtration and dried over CaCl₂ in vacuo. The yield was 0.19 g (42%). Other complexes were prepared under identical conditions, and yield varied in the range 45–50%. Anal. Calcd for C₂₀H₂₀N₈I₂Hg (**4a**): C, 29.03; H, 2.42; N, 13.55. Found: C, 29.15; H, 2.49; N, 13.40. Calcd for C₂₂H₂₄N₈I₂Hg (**4b**): C, 30.89; H, 2.81; N, 13.11. Found: C, 30.97; H, 2.90; N, 13.05. Calcd for C₂₂H₂₄N₈I₂Hg (**5a**): C, 30.89; H, 2.81; N, 13.11. Found: C, 30.93; H, 2.72; N, 13.15. Calcd for C₂₄H₂₈N₈I₂Hg (**5b**): C, 32.63; H, 3.17; N, 12.69. Found: C, 32.70; H, 3.10; N, 12.60. Calcd for C₃₂H₂₈N₈I₂Hg (**6a**): C, 39.24; H, 2.86; N, 11.45. Found: C, 39.17; H, 2.90; N, 11.50. Calcd for C₃₄H₃₂N₈I₂Hg (**6b**): C, 40.53; H, 3.18; N, 11.13. Found: C, 40.45; H, 3.12; N, 11.05.

3.3.b. Synthesis of [Hg(HaaiMe)(μ-I)I]₂ (10a**).** 1-Methyl 2-(phenylazo)imidazole (0.1 g, 0.54 mmol) in MeOH (10 mL) was added dropwise to a 2-methoxyethanol solution (5 mL) of HgI₂ (0.22 g, 0.48 mmol), and the solution was refluxed for 1 h. It was then cooled, filtered, and left undisturbed for 1 week. Bright orange-red crystals were obtained by slow evaporation. The crystals were

Table 6. Summarized Crystallographic Data for [HgI₂][Pai-Me]₂ (**4a**), [Hg(Pai-Me)(*μ*-I)(I)]₂ (**10a**), and [Hg(Tai-CH₂Ph)(*μ*-I)(I)]₂ (**12b**)

param	4a	10a	12b
empirical formula	C ₂₀ H ₂₀ N ₈ I ₂ Hg	C ₁₀ H ₁₀ N ₄ I ₂ Hg	C ₁₇ H ₁₆ N ₄ I ₂ Hg
fw	826.83	640.61	730.73
temp (K)	296(2)	294(2)	294(2)
cryst system	monoclinic	triclinic	monoclinic
space group	C2/c	P1	P2 ₁ /n
cryst size (mm ³)	0.20 × 0.10 × 0.10	0.20 × 0.12 × 0.10	0.20 × 0.05 × 0.05
<i>a</i> (Å)	27.539(3)	7.5841(7)	11.6496(13)
<i>b</i> (Å)	6.6508(6)	10.408(1)	14.3615(16)
<i>c</i> (Å)	17.2364(17)	10.506(1)	12.8105(14)
α (deg)	90.00	113.784(1)	90.00
β (deg)	124.911(2)	93.111(2)	109.002(2)
γ (deg)	90.00	99.851(2)	90.00
<i>V</i> (Å ³)	2588.8(4)	740.7(1)	2026.5(4)
<i>Z</i>	4	2	4
μ(Mo Kα) (mm ⁻¹)	8.353	14.544	10.648
θ range	1.8–28.31	2.14–28.31	2.05–28.34
<i>hkl</i> range	−35 ≤ <i>h</i> ≤ 23; −8 ≤ <i>k</i> ≤ 8; −19 ≤ <i>l</i> ≤ 22	−9 < <i>h</i> < 9; −13 < <i>k</i> < 13; −13 < <i>l</i> < 13	−13 < <i>h</i> < 15; −19 < <i>k</i> < 17; −17 < <i>l</i> < 17
<i>D</i> _{calc} (mg m ⁻³)	2.121	2.873	2.395
refine params	141	154	187
tot. reflns	8420	7949	13 566
unique reflns	3121	3519	4921
R ₁ ^a [<i>I</i> > 2σ(<i>I</i>)]	0.0410	0.0302	0.0398
wR ₂ ^b	0.1362	0.0743	0.0529
goodness of fit	0.933	0.989	0.750

^a $R = \sum ||F_o| - |F_c|| / \sum |F_o|$. ^b $wR_2 = [\sum w(F_o^2 - F_c^2)^2 / \sum w(F_o^2)^2]^{1/2}$; $w = 1/[\sigma^2(F_o)^2 + (0.1000P)^2 + (0.0000P)]$ for **4a**, $w = 1/[\sigma^2(F_o)^2 + (0.0420P)^2 + (0.0000P)]$ for **10a**, and $w = 1/[\sigma^2(F_o)^2 + (0.0010P)^2 + (0.0000P)]$ for **12b**, where $P = (F_o^2 + 2F_c^2)/3$.

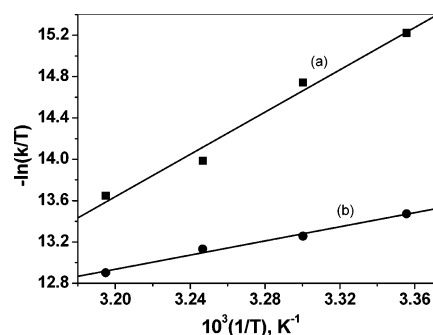


Figure 6. Arrhenius plots of rate constants of the cis-to-trans thermal isomerization of (a) Tai-Me and (b) [Hg(Tai-Me)(*μ*-I)(I)]₂ at different temperatures.

collected by filtration, washed with cold methanol, and dried over CaCl₂ in vacuo. The yield was 0.23 g (74%). Other complexes were prepared under identical conditions, and yield varied in the range 65–75%. Anal. Calcd for C₁₀H₁₀N₄I₂Hg (**10a**): C, 18.73; H, 1.56; N, 8.74. Found: C, 18.65; H, 1.49; N, 8.80. Calcd for C₁₁H₁₂N₄I₂Hg (**10b**): C, 20.17; H, 1.83; N, 8.55. Found: C, 20.08; H, 1.90; N, 8.65. Calcd for C₁₁H₁₂N₄I₂Hg (**11a**): C, 20.17; H, 1.83; N, 8.55. Found: C, 20.12; H, 1.76; N, 8.68. Calcd for C₁₂H₁₄N₄I₂Hg (**11b**): C, 21.54; H, 2.09; N, 8.38. Found: C, 21.70; H, 2.00; N, 8.45. Calcd for C₁₆H₁₄N₄I₂Hg (**12a**): C, 26.79; H, 1.95; N, 7.81. Found: C, 26.66; H, 1.90; N, 7.90. Calcd for C₁₇H₁₆N₄I₂Hg (**12b**): C, 27.92; H, 2.19; N, 7.67. Found: C, 28.05; H, 2.12; N, 7.78.

3.4. X-ray Diffraction Study. The crystallographic data are shown in Table 6. Suitable single crystals of complexes **4a** (0.20 × 0.10 × 0.10 mm³), **10a** (0.20 × 0.12 × 0.10 mm³), and **12b** (0.20 × 0.05 × 0.05 mm³) were mounted on a Siemens CCD diffractometer equipped with graphite-monochromated Mo Kα ($\lambda = 0.71073$ Å) radiation. The unit cell parameters and crystal-orientation matrices were determined for two complexes by least-squares refinements of all reflections. The intensity data were corrected for Lorentz and polarization effects, and an empirical absorption correction were also employed using the SAINT program.²⁴ Data were collected by applying the condition $I > 2\sigma$

(*I*). All these structures were solved by direct methods and followed by successive Fourier and difference Fourier syntheses. Full-matrix least-squares refinements on *F*² were carried out using SHELXL-97 with anisotropic displacement parameters for all non-hydrogen atoms. Hydrogen atoms were constrained to ride on the respective carbon or nitrogen atoms with an isotropic displacement parameters equal to 1.2 times the equivalent isotropic displacement of their parent atom in all cases. Complex neutral atom scattering factors were used throughout for all cases. All calculations were carried out using SHELXS 97,²⁵ SHELXL97,²⁶ PLATON 99,²⁷ and ORTEP-3²⁸ programs.

3.5. Photometric Measurements. Absorption spectra were taken with a Perkin-Elmer Lambda 25 UV/vis spectrophotometer in a 1 × 1 cm quartz optical cell maintained at 25 °C with a Peltier thermostat. The light source of a Perkin-Elmer LS 55 spectrofluorometer was used as an excitation light, with a slit width of 10 nm. An optical filter was used to cut off overtones when necessary. The absorption spectra of the cis isomers were obtained by extrapolation of the absorption spectra of a cis-rich mixture for which the composition is known from ¹H NMR integration. Quantum yields (ϕ) were obtained by measuring initial trans-to-cis isomerization rates (ν) in a well-stirred solution within the above instrument using the equation

$$\nu = (\phi I_0/V)(1 - 10^{-\text{Abs}})$$

where *I*₀ is the photon flux at the front of the cell, *V* is the volume of the solution, and Abs is the initial absorbance at the azobenzene ($\phi = 0.11$ for π - π^* excitation²⁹) under the same irradiation condition.

(24) SMART and SAINT; Bruker AXS Inc.: Madison, WI, 1998.

(25) Sheldrick, G. M. SHELXS 97, Program for the Solution of Crystal Structure; University of Gottingen: Gottingen, Germany, 1997.

(26) Sheldrick, G. M. SHELXL 97, Program for the Solution of Crystal Structure; University of Gottingen: Gottingen, Germany, 1997.

(27) Spek, A. L. PLATON, Molecular Geometry Program; University of Utrecht: Utrecht, The Netherlands, 1999.

(28) Farrugia, L. J. ORTEP-3 for windows. J. Appl. Crystallogr. 1997, 30, 565.

(29) Zimmerman, G.; Chow, L.; Paik, U. J. Am. Chem. Soc. 1958, 80, 3528.

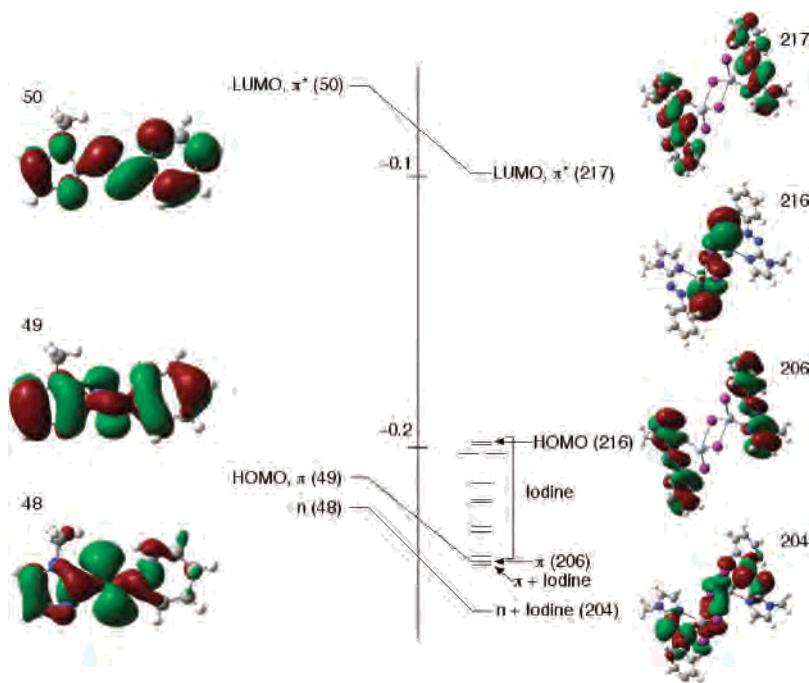


Figure 7. Frontier molecular orbitals of **1a** and **10a**. The ordinate indicates orbital energies in hartrees. The numbers in parentheses indicate molecular orbital numbers. Orbitals of similar symmetries in parts of the ligand are connected.

The thermal cis-to-trans isomerization rates were obtained by monitoring absorption changes intermittently for a cis-rich solution kept in the dark at constant temperatures in the range from 298 to 313 K. The activation energy (E_a) and the frequency factor (A) were obtained from the Arrhenius plot,

$$\ln k = \ln A - E_a/RT$$

where k is the measured rate constant, R is the gas constant, and T is temperature. The values of activation free energy (ΔG^*) and activation entropy (ΔS^*) were obtained through the relationships

$$\Delta G^* = E_a - RT - T\Delta S^*$$

$$\Delta S^* = [\ln A - 1 - \ln(k_B T/h)]/R$$

where k_B and h are Boltzmann's and Planck's constants, respectively.

3.5. DFT Calculations. The density functional theory (DFT) calculations on the crystal structures of **1a**⁹ and **10a** were carried out using the Gaussian 03w program package³⁰ with the aid of the

GaussView visualization program.³¹ The hybrid functional by Becke, B3LYP,³² was used, which include a mixture of Hartree–Fock exchange with DFT exchange–correlation. For C, H, N, and I, we used MIDI! basis functions,³³ as this basis set is applicable to all these elements and includes polarization functions. For Hg, we used the LanL2DZ basis set including Los Alamos effective core potentials.^{34–36}

4. Conclusion

The effect of reaction phase on the synthesis of compounds is examined in this work. Neat reaction between HgI_2 and 1-alkyl-2-(arylazo)imidazole (RaaiR') under microwave irradiation has synthesized $[\text{HgI}_2][\text{RaaiR}'_2]$ in which layers of reactants separately positioned in the crystal structure. In solution phase we have isolated iodo-bridged azoimine-chelated coordination complexes of the composition $[\text{Hg}(\text{RaaiR}')(\mu\text{-I})(\text{I})_2]$. Single-crystal X-ray diffraction study has determined the structure of the complexes. Both ligands and iodo-bridged Hg(II) complexes show photochromism upon UV light irradiation. Quantum yields of trans-to-cis isomerization are determined in toluene for ligands and in MeCN for complexes. The cis-to-trans isomerization is a thermally driven process. The activation energies (E_a 's) of cis-to-trans isomerization have been calculated. The slow rate of isomerization in complexes may be due to higher rotor volume than that of free ligands.

(30) Frisch, M. J.; Trucks, G. W.; Schlegel, H. B.; Scuseria, G. E.; Robb, M. A.; Cheeseman, J. R.; Montgomery, J. A., Jr.; Vreven, T.; Kudin, K. N.; Burant, J. C.; Millam, J. M.; Iyengar, S. S.; Tomasi, J.; Barone, V.; Mennucci, B.; Cossi, M.; Scalmani, G.; Rega, N.; Petersson, G. A.; Nakatsuji, H.; Hada, M.; Ehara, M.; Toyota, K.; Fukuda, R.; Hasegawa, J.; Ishida, M.; Nakajima, T.; Honda, Y.; Kitao, O.; Nakai, H.; Klene, M.; Li, X.; Knox, J. E.; Hratchian, H. P.; Cross, J. B.; Bakken, V.; Adamo, C.; Jaramillo, J.; Gomperts, R.; Stratmann, R. E.; Yazyev, O.; Austin, A. J.; Cammi, R.; Pomelli, C.; Ochterski, J. W.; Ayala, P. Y.; Morokuma, K.; Voth, G. A.; Salvador, P.; Dannenberg, J. J.; Zakrzewski, V. G.; Dapprich, S.; Daniels, A. D.; Strain, M. C.; Farkas, O.; Malick, D. K.; Rabuck, A. D.; Raghavachari, K.; Foresman, J. B.; Ortiz, J. V.; Cui, Q.; Baboul, A. G.; Clifford, S.; Cioslowski, J.; Stefanov, B. B.; Liu, G.; Liashenko, A.; Piskorz, P.; Komaromi, I.; Martin, R. L.; Fox, D. J.; Keith, T.; Al-Laham, M. A.; Peng, C. Y.; Nanayakkara, A.; Challacombe, M.; Gill, P. M. W.; Johnson, B.; Chen, W.; Wong, M. W.; Gonzalez, C.; Pople, J. A. *Gaussian 03*, revision C.02; Gaussian, Inc.: Wallingford, CT, 2004.

(31) Dennington, R., II; Keith, T.; Millam, J.; Eppinnett, K.; Hovell, W. L.; Gilliland, R. *GaussView*, version 3.09; Semichem, Inc.: Shawnee Mission, KS, 2003.

(32) Becke, A. D. *J. Chem. Phys.* **1993**, *98*, 5648.

(33) Easton, R. E.; Giesen, D. J.; Welch, A.; Cramer, C. J.; Truhlar, D. G. *Theor. Chim. Acta* **1996**, *93*, 281.

(34) Hay, P. J.; Wadt, W. R. *J. Chem. Phys.* **1985**, *82*, 270.

(35) Wadt, W. R.; Hay, P. J. *J. Chem. Phys.* **1985**, *82*, 284.

(36) Hay, P. J.; Wadt, W. R. *J. Chem. Phys.* **1985**, *82*, 299.

Acknowledgment. Financial support from the Council of Scientific and Industrial Research (CSIR) and Department of Science & Technology (DST), New Delhi, is gratefully acknowledged. K.K.S. thanks the CSIR for a fellowship.

Supporting Information Available: Crystallographic data in CIF format. This material is available free of charge via the Internet at <http://pubs.acs.org>. Crystallographic data for the structures have

also been deposited with the Cambridge Crystallographic Data Center (CCDC No.: 293801, [HgI₂][HaaiMe]₂ (**4a**); 293802, [Hg-(HaaiMe)(μ -I)(I)]₂ (**10a**); 293803, [Hg(MeaaiCH₂Ph)(μ -I)(I)]₂ (**12b**)). Copies of this information may be obtained free of charge from the Director, CCDC, 12 Union Road, Cambridge CB2 1EZ, U.K. (e-mail, deposit@ccdc.cam.ac.uk, or www.ccdc.cam.ac.uk).

IC061221U